Chemical Science

Accepted Manuscript

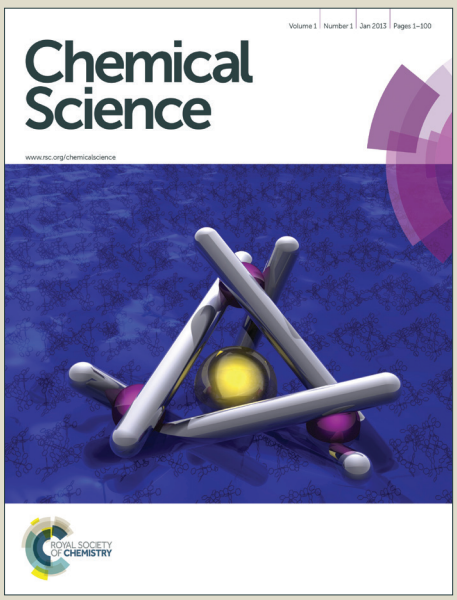

ROYAL SOCIETY OF CHEMISTRY

www.rsc.org/chemicalscience

Journal Name

RSCPublishing

ARTICLE

Diindeno[1,2-*b*:2',1'-*n*]Perylene: a Closed Shell related Chichibabin's Hydrocarbon, Synthesis, Molecular Packing, Electronic and Charge Transport Properties

Cite this: DOI: 10.1039/xoxxoooooox

Received ooth January 2012,
Accepted ooth January 2012

DOI: 10.1039/xoxxoooooox

www.rsc.org/

Kamal Sbargoud,[a] Masashi Mamada,[*b] Jérôme Marrot,[a] Shizuo Tokito[b], Abderrahim Yassar[*c] and Michel Frigoli[*a]

Diindeno[1,2-*b*:2',1'-*n*]perylene, a new derivative of the indenoacene family was synthesized, and its electronic, electrochemical, and electrical properties were investigated. This material has a closed shell electronic configuration which corresponds to a quinoidal structure with a low band gap of 1.35 eV. Molecular packing in the single crystal was studied by single-crystal X-ray structural analysis, and this information was subsequently used in the determination of the charge transfer integrals via density functional theory methods. The charge-carrier transport properties of the diindeno[1,2-*b*:2',1'-*n*]perylene-5,12-dione and Diindeno[1,2-*b*:2',1'-*n*]perylene derivatives were investigated through the fabrication and characterization of field-effect transistors via both vacuum-deposited and solution-processed films, respectively. Diindeno[1,2-*b*:2',1'-*n*]perylene exhibited field-effect behaviour with a hole mobility up to 1.7×10^{-3} cm^2 V^{-1} s^{-1} when the active layer was solution-processed.

Introduction

The design and synthesis of new functional π-conjugated materials is a major issue in the development of next generation of organic optoelectronic devices. Continuous research efforts have contributed to the great advances in materials development, along with innovations and optimizations in the device structure and processing.[1,2] The progresses made are the result of the improvements in fabrication processes and a better understanding of the design rules to yield efficient π-conjugated materials. Tremendous efforts have been focused on the functionalization of known molecules (e.g. thiophene, benzene, fluorene, etc.) with electron-withdrawing or donating group, alternating electron donor and electron deficient building blocks or incorporation heteroatoms into the π-conjugated backbone.[3] However, further improvement of the material performance requires the development of new concept in designing of building blocks and the in-depth understanding of the structure−property relationships. Toward this end, several synthetic approaches have been developed and one promising is the use of quinoidal molecules as a useful building block for constructing functional materials. Quinoidal polycyclic hydrocarbons (QPHs) have been recently the subject of intense researches due to their potential to have an open shell character with fascinating optical, electronic and magnetic properties.[4] Environmentally stable closed shell QPHs are very promising for OFETs and photovoltaic applications due to their inherent planar structure that could improve π−π stacking capability and facilitate charge delocalization and transport. Moreover, the quinoidal π-conjugated system reduces the HOMO-LUMO energy gap by stabilizing more the LUMO energy level than destabilizing the HOMO one compared to their aromatic analogues and show amphoteric redox behaviours, which is a prerequisite for their use as ambipolar semiconductors. Several QPHs have been developed in the recent years such as bisphenalenyls,[5] zethrenes[6] and indenofluorenes.[7] The latter family is of interest due to the ease of their synthesis and tuning their optical and electronic properties with the possibility to fuse two indene units in different fashions into diverse π-conjugated spacer. Considering a benzene group as the conjugated spacer, four isomers with a plan or centre of symmetry have been developed (Fig. 1).[7a-d,f] They have either a central *para*- (**1a**, **1c**), *ortho*- (**1b**) or *metha*-quinomethane (**1d**) unit. Isomers **1a-c** are best described as quinoidal closed shell molecule in the ground state ensuring a good stability whereas **1d** has a little contribution of the singlet biradical canonical structure to the ground-state electronic configuration. The difference between these isomers is best described by considering the number of aromatic sextet between the quinoidal form (closed shell) and the diradical form (open shell) according to Clar's rule. The closed shell **1a-c** has two

aromatic sextets whereas the corresponding open shell has three aromatic sextets.

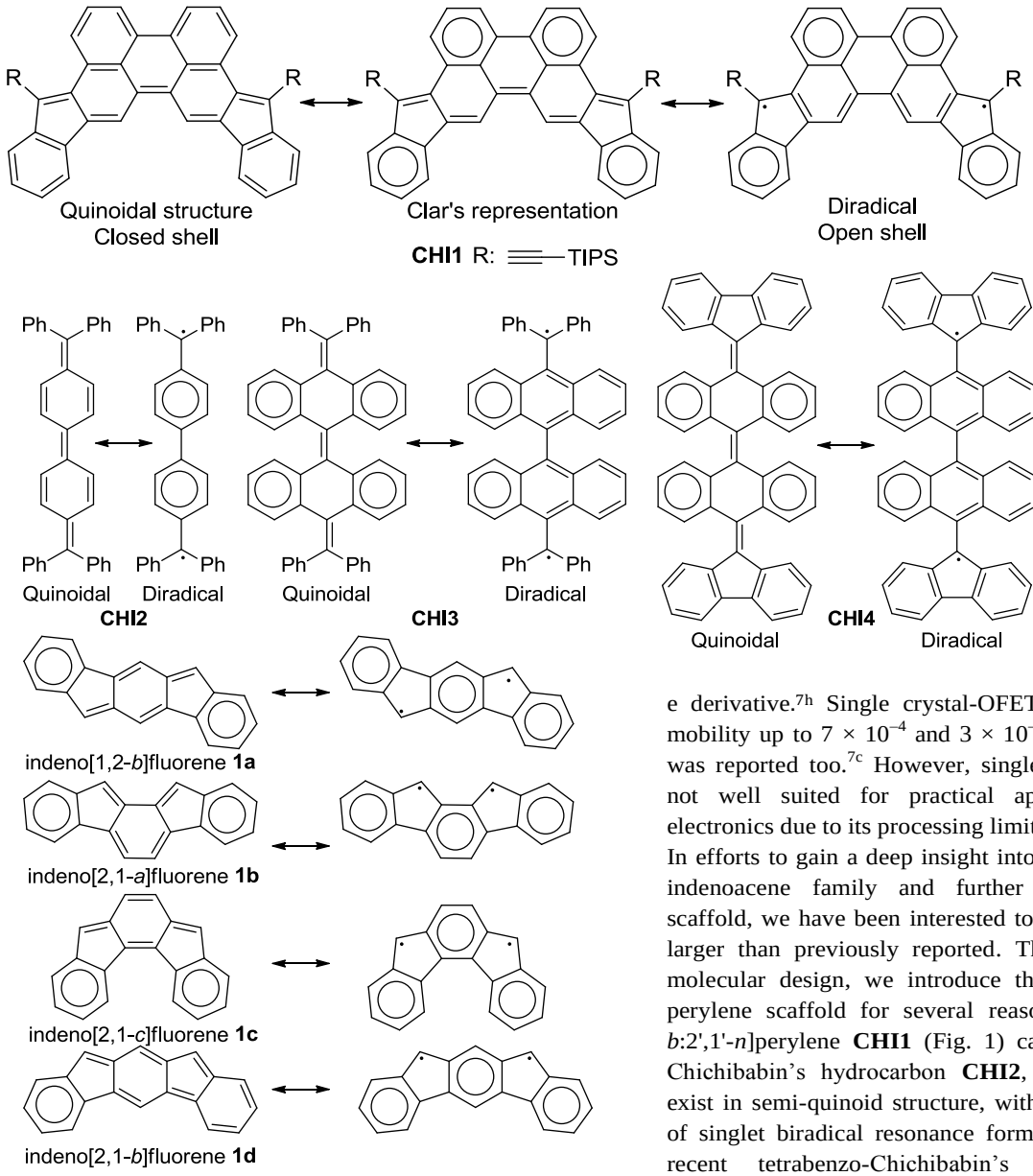

Fig. 1 Chemical and resonance structure of the indenofluorene family, the Chichibabin's **CHI2**, the tetrabenzo-chichibabin's derivatives **CHI3** and **CHI4** and the diindeno[1,2-*b*:2',1'-*n*]perylene **CHI1** reported in this work.

The gain in aromaticity in the corresponding open shell resonance is not enough to compensate the dissociation energy of the two double bonds and the reorganization of the π–electron in the system. For **1d**, the biradical form has two more aromatic sextets compared to the quinoidal one and leads to a little contribution of the biradical resonance in the ground state. The biradical character of molecules belonging to the bisindeno-acene family can simply be anticipated when at least a difference of two aromatic benzenoid sextets between the quinoidal and biradical form is present.

Although the progress made on synthetizing indenofluorene materials with good optical and electronic properties, only three reports describing the organic field effect transistor (OFET) characteristics have been reported. Low carrier mobilities (hole and electron) of 8.2 10^{-6} cm^2 V^{-1} s^{-1} were measured for aryl-substituted derivatives in evaporated thin film.[7b] The low mobilities were attributed to the lack of efficient π-π stacking in the crystal. Higher hole mobility (1.6×10^{-2} cm^2 V^{-1} s^{-1}) was obtained from a preliminary field effect transistor test on the spin-coated thin films of a diindenothienothiophen e derivative.[7h] Single crystal-OFETs with hole and electron mobility up to 7×10^{-4} and 3×10^{-3} cm^2 V^{-1} s^{-1}, respectively was reported too.[7c] However, single crystal devices might be not well suited for practical applications in large area electronics due to its processing limitations.

In efforts to gain a deep insight into electronic structure of the indenoacene family and further expand their versatility scaffold, we have been interested to other conjugated systems, larger than previously reported. Thus, from a viewpoint of molecular design, we introduce the indeno groups into the perylene scaffold for several reasons: a) The diindeno[1,2-*b*:2',1'-*n*]perylene **CHI1** (Fig. 1) can be regarded as a fixed Chichibabin's hydrocarbon **CHI2**, which recently found to exist in semi-quinoid structure, with a significant contribution of singlet biradical resonance form (Fig. 1).[8] Moreover, two recent tetrabenzo-Chichibabin's derivatives have been disclosed, displaying either a closed- (**CHI3**) or open shell (**CHI4**) electronic configuration (Fig. 1).[9] For these cases, even though the closed shell form has two more aromatic sextets than the open shell one, the electronic configuration could be tuned by substituent effect on the thermodynamic stabilization of the diradical form. **CHI1** can be viewed also as an extension of the closed shell indeno[2,1-*c*]fluorene **1c** derivative in which the central phenylene group is replaced by a *p*-biphenylene linker. Therefore, the extension of the π-conjugation should lead to a low band gap material; b) According to Clar's rule, the quinoidal structure of **CHI1** and the biradical resonance form have the same number of aromatic sextets (Fig. 1). So, in line with the relationship between the structure and the electronic configuration known for the indenofluorene family as described above, **CHI1** should have a closed shell configuration ensuring

a good stability. Thus, it was of high interest to assess the electronic configuration of **CHI1** in order to a have better understanding of the relationship between the structure and the electronic configuration; c) The perylene scaffold should promote good π-π overlap, thus a good charge transport properties could be expected.

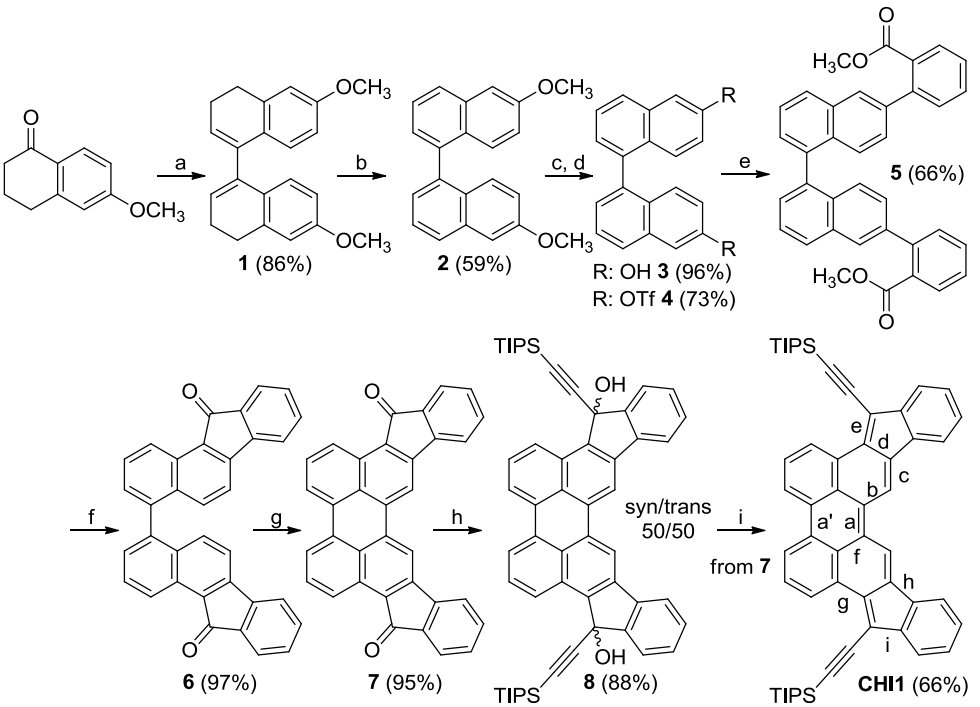

Scheme 1 Synthetic path of **CHI1**: (a) Zn, TMSCl, HCl, THF -50°C; (b) 1) tritylfluoroborate, CH_2Cl_2, 0°C; 2) NEt_3, rt; (c) BBr_3, CH_2Cl_2, 0°C; (d) OTf_2, pyridine, CH_2Cl_2, 0°C; (e) 2-methoxycarbonylphenylboronic acid, $Pd(PPh_3)_4$, K_3PO_4, DMF, 95°C; (f) CH_3SO_3H, 75°C; (g) K_2CO_3, ethanolamine, 160°C; (h) TIPSCCLi, THF, 0°C – rt; (i) $SnCl_2$, toluene, 120°C.

Herein, we describe an efficient synthetic method to prepare **CHI1** in which the conjugation of the central perylene core is extended by the annelation of the two indene units. To address processability issue, we introduce the (triisopropylsilyl)acetylene group to both improve solvent solubility, stabilizing the structure by electronic effect, increase π-π interactions and improved charge transport properties.[10] An overview of the synthetic procedures is presented first, and then the electronic and electrical properties of these new materials, including their absorption, electrochemical properties, molecular packing and charge transport behaviour, are developed and discussed.

Results and discussions

The synthetic path used to synthesize **CHI1** followed the same strategy than the synthesis of indenofluorene derivatives that relies on the synthesis of a diketone molecule which is consequently reacted with an appropriate lithium derivative followed by a dehydroxylation reaction (Scheme 1). However, the preparation of **CHI1** was more challenging than that of the other indenoacene derivatives reported so far due to the need of the construction of the perylene core with suitable functionalities. One of the simplest and efficient methodology to construct the perylene moiety is based on a base-promoted cyclodehydrogenation reaction of 1,1'-binaphthyl derivatives bearing withdrawing substituents at the peri-position using K_2CO_3 and ethanolamine.[11,12] We assumed that this procedure should work well with the ketone groups positioned in para of the reactive carbons in which the cyclisation occurs. Consequently, the critical reaction involved the preparation of the diindeno[1,2-*b*:2',1'-*n*]perylene-5,12-dione **7** from the 1,1'-binaphthyl derivative **6** namely 11*H*,11'*H*-[4,4'-bibenzo[*a*]fluorene]-11,11'-dione.

The synthesis starts with the dimerization of 6-methoxytetralone using zinc in presence of protic chlorotrimethylsilane.[13] It should be noted that a simple filtration under silica gel pad, the 6,6'-dimethoxy-3,3',4,4'-tetrahydro-1,1'-binaphthalene **1** decomposes partially to the corresponding hexahydrobenzo[*j*]fluoranthene derivative involving a ring closure with the formation of 5-membered ring. Nevertheless, compound **1** is isolated with a good quality and a yield of 86% after workup without purification. The aromatisation of compound **1** could not be carried out with classical oxidant such DDQ and *p*-chloranil. Thus, the 6,6'-dimethoxy-1,1'-binaphthalene **2** was obtained in 59% yield using trityl fluoroborate instead. Treatment of **2** with BBr_3 yielded quantitatively the corresponding dihydroxybinaphtalene **3**, followed by a triflation reaction carried out in a classical manner afforded the corresponding 1,1'-binaphthalene triflate **4**. The palladium-catalysed Suzuki–Miyaura cross-coupling reaction between the bis-triflate **4** and 2-methoxycarbonylphenylboronic acid gave the compound **5** in 66% yield. The cyclization of the ester group was carried out with methanesulfonic acid to furnish the dione **6** in quantitative yield. The cyclodehydrogenation of **6** was efficiently obtained with K_2CO_3/ethanolamine upon heating to give the desired parent diindenoperylene-5,12-dione **7**. The addition of the lithium-triisopropylsilylacetylene to **7** induced the formation of diols **8** in excellent yield. The corresponding syn-/anti-diastereoisomers have been easily separated under column chromatography since the difference of the retention factor (Rf) is large. The Rf values were found to be 0.39 and 0.09 in a mixture petroleum ether/dichloromethane for the first and second diastereoisomer respectively. The $SnCl_2$-mediated dehydroxylation of the resulting mixture of diols has been carried out in toluene at 120 °C for 1h leading to a dark blue solution. Longer time induces the formation of *by*-products. The targeted molecule **CHI1** has been isolated in 66% yield over two steps after purification under silica gel column in a

mixture of toluene/petroleum ether (50/50). Due to the very low solubility of compounds **6** and **7** in common solvents, only ^{1}H NMR spectrum of **7** could be recorded. However, these two molecules were characterized by infrared spectroscopy and X-ray crystallography and elemental analysis.[14,15] Infrared spectra of the compounds **7** and **8** showed characteristic peaks of the C=O stretching belonging to an arylketone at 1695 cm^{-1} and 1691 cm^{-1}, respectively (see ESI). Other signals, related to the formation of a H-bonded carbonyl group structure are detected at 1601 cm^{-1} and 1579 cm^{-1} for **7** and 1605 cm^{-1} and 1579 cm^{-1} for **8**. The targeted molecule **CHI1** was fairly soluble in common organic solvents and was characterized by ^{1}H NMR, infrared spectroscopy, elemental analysis and X-ray crystallography (see ESI).[16]

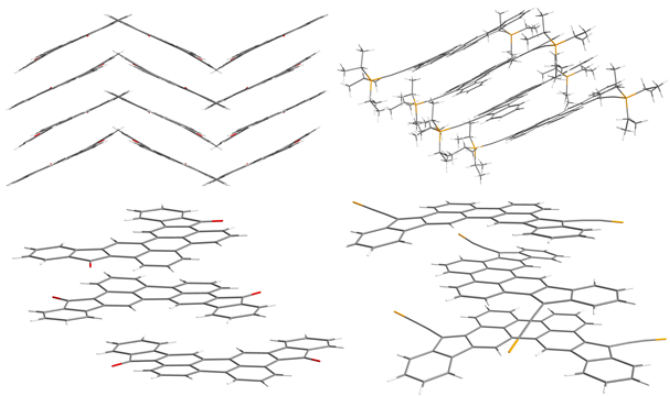

Fig. 3 Crystal structures and molecular packing of **7** (left) and **CHI1** (right). The isopropyl group was removed for clarity.

The ^{1}H NMR spectrum of **CHI1** shows sharp signal at room temperature and consequently supports the quinoidal structure in the ground state (see ESI). Crystals suitable for X-ray structure analysis were obtained by recrystallization from chloroform for **7** and benzene for **CHI1** (Fig. 3). Both compounds gave crystals with orthorhombic symmetry. **7** and **CHI1** crystallize in the P*bcn* and P*bca* space group, respectively. It should be noticed that **CHI1** co-crystallize with benzene molecule in a ratio 2 for 1. The selected bond lengths of the π-part, which change significantly between **7** and **CHI1**, are listed in Tab. 1 together with those of Chichibabin's molecules **CHI2** and **CHI3**.

Tab. 1 Comparison of bond lengths of **7** and **CHI1** in crystals and calculated

Bond (Å)	7	7[a] (DFT	CHI1	CHI1[a,b] (DFT)	CHI2[c]	CHI3[d]
a	1.467 (3)	1.474	1.406 (5)	1.414	1.448 (4)	1.350 (8)
a'	1.466 (4)	1.474	1.470 (5)	1.462		
b	1.389 (3)	1.400	1.435 (5)	1.439	1.420 (3)	1.496 (6)
c	1.388 (3)	1.394	1.352 (5)	1.359	1.372 (3)	1.401 (5)
d	1.378 (4)	1.393	1.450 (5)	1.452	1.429 (3)	1.482 (6)
e	1.484 (4)	1.497	1.386 (5)	1.393	1.420 (3)	1.342 (6)
f	1.435 (3)	1.434	1.451 (5)	1.447		
g	1.413 (4)	1.414	1.438 (5)	1.449		
h	1.484 (4)	1.485	1.467 (5)	1.464		
i	1.496 (4)	1.497	1.467 (5)	1.472		

a) Calculated by DFT methods at the B3LYP/6-31G(d,p) level using the Gaussian 09 program; [17] b) The TIPS groups of **CHI1** were omitted and hydrogen atoms were used in their place; c) Taken from ref. 8b; d) Taken from ref. 9.

For comparison, the theoretical bond lengths of **7** and **CHI1** without the TIPS group**s** estimated by DFT calculations are given in Table 1 as well. The calculated bond lengths of both molecules agree well with those of the experimental data within experimental errors. The crystal structure of **7** shows characteristics of the perylene scaffold. By contrast, the structure of **CHI1** shows clearly a bond-length alternation in the π-skeleton: the bonds denoted by a, c, and e have substantial double-bond character, whereas the bonds denoted by b, d and f-i have rather a single-bond character (Tab. 1; Scheme 1). The bonds lengths (d,e,h,i) of the five-membered ring are typical for the closed shell quinoidal indenofluorene derivatives. The shortening of the bond length a (1.406(5) Å) compared to the bond length a' (1.470(5) Å) and a (1.448(4) Å) in the corresponding Chichibabin's molecule **CHI2** is significant but longer to the one observed for **CHI3** (1.350(8) Å). The bond length of a in **CHI1** is longer than a typical double bond which is ascribed to the steric hindrance between the two hydrogens located at the bay region of the perylene core which is below the sum of their van der Waals radii. The bond lengths suggest unambiguity that **CHI1** has a quinoidal electronic configuration in the ground state. It should be noticed that **CHI1** is stable in a non-degassed toluene solution for more than six months in the dark and for 1 week in the laboratory environment. Moreover, the analyse of nucleus independent chemical shift (NICS) values, NICS(1) (NICS(1)zz),[18] for the five-membered- and the quinoidal adjacent rings were −1.80 (5.25) and −1.66 (4.04), respectively, indicates a weak antiaromatic character. In comparison, the isomer **1c** shows a stronger antiaromatic character with values for the five-membered ring of 4.18 (21.76) and 0.57 (9.61) for the quinoidal ring (see ESI).

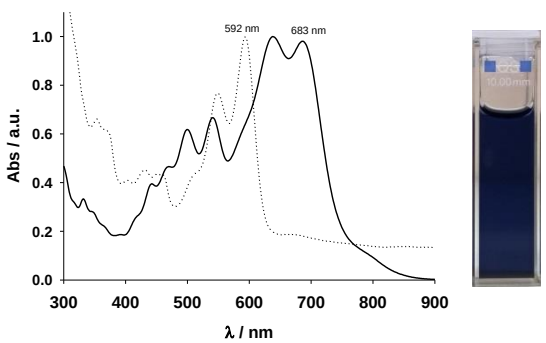

Fig. 4 Absorption spectra of **7** (dotted line) and **CHI1** (bold line) in toluene. Insert is the photo of **CHI1**.

Compounds, **7** and **CHI1,** arrange into 1-D columnar stack in which molecules form pairwise slipped stacks. The distance between average planes within the pair is 3.37 Å and 3.39 Å and 3.19 Å and 3.41 Å within adjacent pairs for **7** and **CHI1** respectively. Lateral slip of the π-conjugated system was found to be 1.56 Å and 2.04 Å in the pair and 5.14 Å and 2.00 Å between pairs for **7** and **CHI1** respectively. In **7**, 1D-columns forms layers of parallel columns and each alternate layer is twisted to each other. The dihedral angle between the average planes is 54.28°. The 1D-columns interact through hydrogen

bonds (CH-O) of lengths 2.47 Å into the layers and 2.43 Å within the layers. For **CHI1**, the 1D-columns are separated from adjacent columns by the TIPS groups and benzene molecules.

The charge-transfer processes are impacted by the geometry and molecular packing as well as by the intermolecular electronic coupling. An accurate understanding of all these molecular characteristics is an important prerequisite for the design and selection of appropriate molecules as well as for optimizing the performance of the devices. Therefore, we have performed a study of the transfer integral in the dimer of **7** and **CHI1** (Fig. S2 in ESI) using the Amsterdam Density Functional (ADF) program package. Compound **7** exhibits a large intra-dimer transfer integral, on the order of 142 meV and 4.3 meV for inter-dimer contacts. Although compound **CHI1** displays a slightly different crystalline structure, the calculated transfer integral (5.4 meV) is much lower than the transfer integral of **7**. Hence, this study of the transfer integral shows clearly that intra-columnar direction is a favourable direction for charge transport.

UV/visible spectra of **7** and **CHI1** are depicted in Fig. 4. Compound **7** was very insoluble in commons solvents even at a concentration of 2×10^{-5} mol.L^{-1}. At this concentration, the spectrum shows a maximum wavelength at 592 nm and a diffusion band indicating the presence of aggregates. Compound **CHI1** displays strong blue colour in toluene solution. The UV-vis spectrum of **CHI1** exhibits strong acene-like vibronic features in the visible energy range that extends into the near-IR region (900 nm), with a lowest energy λ_{max} at 683 nm.

Cyclic voltammetry and square wave voltammetry (SQW) were used to investigate the electrochemical behaviour and probe the HOMO/LUMO levels of **CHI1** (Fig. 5). Compound **CHI1** showed amphoteric redox behaviour and exhibits two reversible oxidation and reduction peaks which are typical for indenofluorene derivatives. In SQW, compound **CHI1** displayed two oxidation peaks at 0.5, 1.1 V and two reduction peaks, E_{red} at -1.1 and -1.2 V (vs. Ag/AgNO$_3$) using the Fc/Fc$^+$ couple as internal standard. The onset potentials of the first oxidation and reduction peaks are 0.35 and – 1 V respectively. HOMO and LUMO levels were estimated from the onset potentials and converted to the vacuum scale according to the formula of HOMO = -($E_{ox\text{-}onset}$ + 4.8) eV, LUMO = -($E_{red\text{-}onset}$+ 4.8) eV.[19] According to that, HOMO and LUMO levels were found to be at -5.15 and -3.80 eV. Interestingly, **CHI1** and the TIPS-acetylene functionalised **1c** have similar LUMO level (4.02 eV for **1c**). The extension of the conjugation of the central core and the number of aromatic rings in **CHI1** compared to **1c** (HOMO: 5.75 eV) leads to an increase of the HOMO level by 0.60 eV.

The charge transport properties of diindeno[1,2-*b*:2',1'-*n*]perylene-5,12-dione (**7**) and diindenoperylene (**CHI1**) were investigated in bottom-gate/top-contact (BG/TC) and top-gate/bottom-contact (TG/BC) organic field-effect transistor geometries (details of the device fabrication are provided in the ESI, Fig. S3).

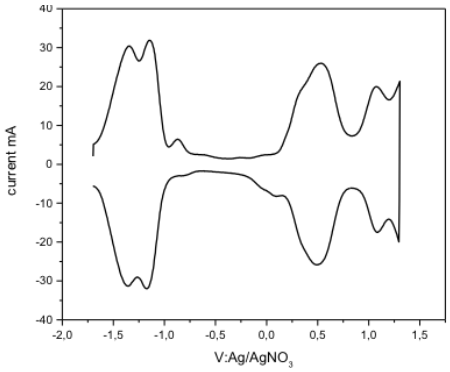

Fig. 5 Square wave voltammogram of **CHI1** in dichloromethane solution, scan rate 60 mV/s, step potential, 50 mV; square-wave frequency, 1 Hz; and square-wave amplitude 10 mV.

Both materials **7** (vacuum-deposited) and **CHI1** (solution-processed film) exhibited measurable hole mobility and showed moderate charge-transport behaviour. Fig. S4 in ESI shows the transfer and output characteristics of an OFET. A hole mobility of 2×10^{-5} cm^2 V^{-1} s^{-1} was extracted from I-V output characteristic for material **7**. When the substrate pre-set temperatures were increased, the device performances of **7** dramatically decreased, and no field effect was detected at T_{sub} = 90°C. The low charge carrier mobility of **7** is may be due to unfavorable orientation of the crystallites and crystallite alignments with respect to the substrate, as evidenced by preliminarily investigation of crystallite orientation of the films using grazing incidence X-ray diffraction. Moreover, the poor performance of this compound might be also attributed to a discontinuous morphology consisting of a spherical structure possibly hindering the charge transport by numerous grain boundaries, as evidenced by atomic force microscopy (AFM) observations, (Fig. S5 in ESI). The bottom gate and top contact (BG/TC) OFET device for thin film of **CHI1** spin-coated from 0.3 wt% chloroform solution showed a hole mobility of 7.3×10^{-4} cm^2 V^{-1} s^{-1} (Fig. S6 and S7 in ESI). The OFET devices of **CHI1** were optimized and a slightly better mobility of 1.7×10^{-3} cm^2 V^{-1} s^{-1} was obtained for the drop-casting thin film with the TG/BC configuration (Fig. 7).

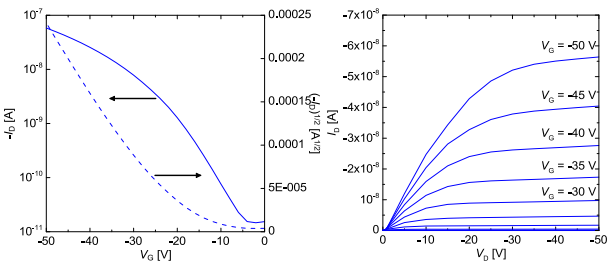

Fig. 7 (a) Transfer and (b) output characteristics of TG/BC device of **CHI1** deposited by drop-casting from 0.2 wt% solution in mesitylene with 0.05 wt% of PS.

The *d*-spacing obtained from the first reflection peak of the out-of-plane X-ray diffraction (XRD) pattern of **CHI1** thin film deposited on HMDS-treated SiO_2 substrate is 16.3 Å (2θ =

5.43°), which may be indexed as (102) based on the solved crystallographic structure of **CHI1**. The in-plane XRD of **CHI1** thin film shows a reflection peak at 2θ = 26.0° (*d*-spacing of 3.42 Å) (Fig. S8 in ESI), which corresponds to a d-spacing of π-π stacking distances between the indenoperylene cores in the crystal (3.39-341 Å in the bulk single crystal). The surface morphology of **CHI1** deposited on HMDS-treated SiO_2 and PVP substrate using different condition process was investigated using AFM.

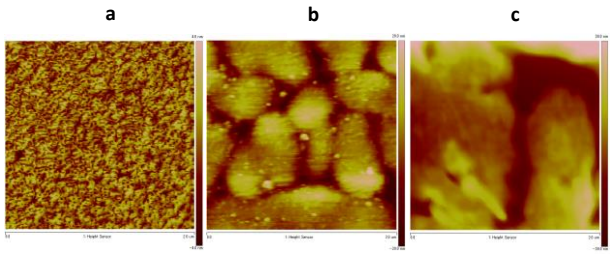

Fig. 8 AFM images (2 μm × 2 μm) of thin films of **CHI1** deposited by (a) spin-coating from the chloroform solution on HMDS-treated SiO_2 substrate, (b) drop-casting from the mesitylene solution on PVP substrate, and (c) drop-casting from the mesitylene solution with PS on PVP substrate.

As shown in Fig. 8, the film surface morphology is strongly affected by processing conditions, in particular on the HMDS-treated SiO_2 (Fig. 8a); the film shows a poor morphological order. On the other hand, on PVP substrates (Fig. 8b,c), the long-range order appears to be considerably improved and the films are characterized by the presence of larger circular islands. Consequently, the device performance under different processing conditions is mainly affected by the changes in the surface morphology, as shown by AFM measurements.

Conclusions

In summary, we have developed an efficient method to prepare a new extended indenoacene derivative in which the two indene groups were introduced into a central perylene core. From a synthetic point of view, the base-promoted cyclodehydrogenation reaction of 1,1'-binaphthyl derivative, bearing ketone groups positioned in para of the reactive carbons in which the cyclisation occurs, using K_2CO_3 and ethanolamine, is an efficient and versatile method to build up the functionalized perylene core. The novel diindeno[1,2-*b*:2',1'-*n*]perylene **CHI1** has a closed shell electronic configuration in the ground state which confirms that the closed-or open shell character of indenoacene derivatives can be expected just by looking at the difference of the number of aromatic sextets between these two mesomeric forms. The diindeno[1,2-*b*:2',1'-*n*]perylene has a quinoidal structure with a broad absorption from 400 nm up to 900 nm and a band gap of 1.35 eV and packed into 1-D columnar stack in the crystal. The best OFET performance with mobility up to 1.7×10^{-3} cm^2 V^{-1} s^{-1} has been found in devices based on solution processed thin films with the TG/BC configuration. This result constitutes one of the rare values obtained for QPHs.

Acknowledgements

The authors thank the LABEX CHARMMMAT for support of this research and Dr. H. Korri-Youssoufi from ICMMO-UMR-CNRS 8182, Université Paris-Sud for performing the electrochemistry measurements. We also thank the Grant-in-Aid for Young Scientists (B) (26810106) from the Japan Society for the Promotion of Science (JSPS), the Japan Regional Innovation Strategy Program by the Excellence (creating international research hub for advanced organic electronics) of Japan Science and Technology Agency (JST), and by the Ministry of Education, Culture, Sports, Science and Technology, Japan.

Notes and References

[a] UMR CNRS 8180, UVSQ, Institut Lavoisier de Versailles, 45 avenue des Etats-Unis, 78035 Versailles Cedex, France. E-mail: michel.frigoli@uvsq.fr
[b] Graduate School of Science and Engineering, Yamagata University, Yonezawa, Yamagata, 992-8510 Japan. E-mail: mamada@yz.yamagata-u.ac.jp
[c] UMR CNRS 7647, LPICM-École Polytechnique, 91128 Palaiseau Cedex, France. E-mail: abderrahim.yassar@polytechnique.edu

Electronic Supplementary Information (ESI) available: See DOI: 10.1039/b000000x/

1. Z. Sun, Q. Ye, C. Chi and J. Wu, *Chem. Soc. Rev*., 2012. **41**, 7857.
2. Y. Diao, L. Shaw, Z. Bao and S. C. B. Mannsfeld, *Energy Environ. Sci*., 2014, **7**, 2145.
3. *Handbook of Thiophene-Based Materials: Applications in Organic Electronics and Photonics*. John Wiley & Sons, Ltd, Chichester, UK. ed. 2009.
4. (*a*) Z. Sun and J. Wu, *J. Mater. Chem*., 2012, **22**, 4151; (*b*) A. Shimizu, Y. Hirao, T. Kubo,M. Nakano, E. Botek and B. Champagne, AIP Conf. Proc., 2012, **1504**, 399; (*c*) Z. Sun, Z. Zeng and J. Wu, *Chem.–Asian. J*., 2013, **8**, 2894; (*d*) M. Abe, *Chem. Rev*., 2013, **113**, 7011; (*f*) Z. Sun and J. Wu, *Pure Appl. Chem*., 2014, **86**, 529; *(e)* T. Kubo, *Chem. Lett.*, 2015, *44*, 111.
5. (*a*) T. Kubo, A. Shimizu, M. Sakamoto, M. Uruichi, K. Yakushi, M. Nakano, D. Shiomi, K. Sato, T. Takui, Y. Morita, and K. Nakasuji, *Angew. Chem*., Int. Ed. 2005, **44**, 6564; (*b*) M. Chikamatsu, T. Mikami, J. Chisaka, Y. Yoshida, R. Azumi and K. Yase, *Appl. Phys. Lett*., 2007, **91**, 043506; (*c*) S. A. Shimizu, M. Uruichi, K. Yakushi, H. Matsuzaki, H. Okamoto, M. Nakano, Y. Hirao, K. Matsumoto, H. Kurata and T. Kubo, *Angew. Chem., Int. Ed*., 2009, **48**, 5482; (*d*) A. Shimizu, T. Kubo, M. Uruichi, K. Yakushi, M. Nakano, D. Shiomi, K. Sato, T. Takui, Y. Hirao, K. Matsumoto, H. Kurata, Y. Morita and K. Nakasuji, *J. Am. Chem. Soc*., 2010, **132**, 14421; (*e*) A. Shimizu, Y. Hirao, K. Matsumoto, H. Kurata, T. Kubo, M. Uruichi and K. Yakushi, *Chem. Commun*., 2012, **48**, 5629.
6 (*a*) Z. Sun, Z. Zeng, and J. Wu, *Acc. Chem. Res*., 2014. **47**, 2582; (*b*) Z. Sun, S. Lee, K. Park, X. Zhu, W. Zhang, B. Zheng, P. Hu, Z. Zeng, S. Das, Y. Li, C. Chi, R. Li, K. Huang, J. Ding, D. Kim and J. Wu, *J. Am. Chem. Soc*., 2013, 135, 18229; (*c*) Z. Sun and J. Wu, *J. Org. Chem*., 2013, **78**, 9032; (*d*) L. Shan, Z.-X. Liang, X.-M. Xu, Q. Tang and Q. Miao, *Chem. Sci*., 2013, **4**, 3294; (*e)* J. L. Zafra, R. C. Gonz´alez Cano, M. C. R. Delgado, Z. Sun, Y. Li, J. T. Lopez

Navarrete, J. Wu and J. Casado, *J. Chem. Phys*., 2014, **140**, 054706; (*f*) Y. Li, K.-W. Huang, Z. Sun, R. D. Webster, Z. Zeng, W. D. Zeng, C. Chi, K. Furukawa and J. Wu, *Chem. Sci*., 2014, **5**, 1908.

7. (*a*) D. T. Chase, B. D. Rose, S. P. McClintock, L. N. Zakharov and M. M. Haley, *Angew. Chem., Int. Ed*., 2011, **50**, 1127; (*b*) A. Shimizu and Y. Tobe, *Angew. Chem., Int. Ed*., 2011, **50**, 6906; (*c*) D. T. Chase, A. G. Fix, S. J. Kang, B. D. Rose, C. D. Weber, Y. Zhong, L. N. Zakharov, M. C. Lonergan, C. Nuckolls and M. M. Haley, *J. Amer. Chem. Soc*., 2012, **134**, 10349. (*d*) A. G. Fix, P. E. Deal, C. L. Vonnegut, B. D. Rose, L. N. Zakharov and M. M. Haley, *Org. Lett*., 2013, **15**, 1362; (*e*) B. D. Rose, C. L. Vonnegut, L. N. Zakharov and M. M. Haley, *Org. Lett*., 2013, **14**, 2426; (*f*) A. Shimizu, R. Kishi, M. Nakano, D. Shiomi, K. Sato, T. Takui, I. Hisaki, M. Miyata and Y. Tobe, *Angew. Chem., Int. Ed*., 2013, **52**, 6076; (*g*) H. Miyoshi, S. Nobusue, A. Shimizu, I. Hisaki, M. Miyatab and Y. Tobe, *Chem. Sci*., 2014, **5**, 163; (*h*) B. S. Young, D. T. Chase, J. L. Marshall, C. L. Vonnegut, L. N. Zakharov and M. M. Haley, *Chem. Sci*., 2014, **5**, 1008; (*i*) X. Shi, P. Mayorga Burrezo, S. Lee, W. Zhang, B. Zheng, G. Dai, J. Chang, J. T. Lopez Navarrete, K-W Huang, D. Kim, J. Casado and Chunyan Chi, *Chem. Sci*., 2014, **5**, 4490; (*j*) D. Luo, S. Lee, B. Zheng, Z. Sun, W. Zeng, K-W. Huang, K. Furukawa, D. Kim, R. D. Webster and J. Wu, *Chem. Sci*., 2014, **5**, 4944; (*k*) S. Nobusue, H. Miyoshi, A. Shimizu, I. Hisaki, K. Fukuda, M. Nakano and Y. Tobe, *Angew. Chem., Int. Ed*., 2015, 54, 2090.
8. (*a*) P. Ravata and M.Baumgarten, *Phys. Chem. Chem. Phys*., 2015, **17**, 983; (*b*) L. K. Montgomery,J. C. Huffman, E. A. Jurczak, and M. P. Grendze, *J. Am. Chem. Soc*., 1986, **108**, 6004.
9. Z. Zeng, Y. M. Sung, N. Bao, D. Tan, R. Lee, J. L. Zafra, B. S. Lee, M. Ishida, J. Ding, J. T. López Navarrete, Y. Li, W. Zeng, D. Kim, K.-W. Huang, R. D. Webster, J. Casado and J. Wu, *J. Amer. Chem. Soc*., 2012, **134**, 14513.
10 (*a*) J. E. Anthony, J. S. Brooks, D. L. Eaton and S. R. Parkin, *J. Am. Chem. Soc*., 2001, **123**, 9482; (*b*) J. E. Anthony, *Chem. Rev*., 2006, **106** , 5028.
11. F. Nolde, J. Qu, C. Kohl, N. G. Pschirer, E. Reuther and K. Müllen, *Chem. Eur. J*., 2005, **11**, 3959.
12 L. Andrew, B. VanVeller and T. M. Swager, *Synlett*, 2010, 3045.
13 A. K. Banerjee, M. C. Sulbaran de Carrasco, C. S. V. Frydrych-Houge, W. B. J. Motherwell, *Chem. Soc. Chem. Commun*., 1986, 1803.
14 Crystallographic data for **6**: $C_{34}H_{18}O_2$, *Mw* = 458.48, *T* = 296(2) K, Monoclinic , space group C2, *a* = 13.707(2) Å, *b* = 6.3468(10) Å, *c* = 13.269(3) Å, α = 90°, β = 103.472(8)°, γ = 90°, *V* = 1122.5(3) Å^3, *Z* = 2, θ_{max} = 30.70°, 6280 reflections, 1865 independent reflections, *R1* = 0.0302, *wR2* = 0.1011 , CCDC 1050080.
15 Crystallographic data for **7**: $C_{34}H_{16}O_2$, *Mw* = 456.47, *T* = 296(2) K, Orthorhombic , space group *Pbcn*, *a* = 18.9562(15) Å, *b* = 15.4930(15) Å, *c* = 14.8168(14) Å, α = 90°, β = 90°, γ = 90°, *V* = 4351.5(7) Å^3, *Z* = 8, θ_{max} = 25.082°, 101569 reflections, 3842 independent reflections, *R1* = 0.0651, *wR2* = 0.1611, CCDC 1050081.
16 Crystallographic data for **CHI1**: $C_{56}H_{58}Si_2$, 0.5(C_6H_6), Mw = 826.25, T = 200(2) K, Orthorhombic , space group Pbca, *a* = 34.006(2) Å, *b* = 7.6167(5) Å, *c* = 36.832(2) Å, α = 90°, β = 90°, γ = 90°, *V* = 9540.0(10) Å^3, *Z* = 8, θ_{max} = 25.082°, 144325 reflections, 8431 independent reflections, *R1* = 0.0778, *wR2* = 0.1623, CCDC 1050082.
17 Frisch, M. J. et al. Gaussian 09, revision C.01; Gaussian, Inc.: Wallingford, CT, 2010; see ESI for full references.
18 H. Fallah-Bagher-Shaidaei, C. S. Wannere, C. Corminboeuf, R. Puchta, and P. v. R. Schleyer, *Org. Lett.*, **2006**, *8*, 863.
19 J. Pommerehne, H. Vestweber, W. Guss, R. F. Mahrt, H. Bässler, M. Porsch, J. Daub, *Adv. Mater*., **1995**, *7*, 551.